Targeting ACSS2 activity suspends the formation of chemoresistance through suppressed histone H3 acetylation in human breast cancer

Xiaoxi Shui
Hebei Normal University
Liying Tian
Hebei Chemical Engineering and Pharmaceutical College
Yuepeng Zhou
Hebei University of Chinese Medicine
Baohua Zhao
zhaobaohua@hebtu.edu.cn

Hebei Normal University

Research Article

Keywords: short-chain fatty acids, acetyl-CoA synthetase short-chain family member 2, histone acetylation, ATP-binding cassette transporters, chemoresistance, breast cancer

Posted Date: February 21st, 2024

DOI: https://doi.org/10.21203/rs.3.rs-3964435/v1

Additional Declarations: No competing interests reported.

Abstract

Histone hyperacetylation is a prevalent occurrence in neoplastic cells within tumors, arising from the coordinated interplay of various biological processes. This phenomenon relies on the robust modulation of gene expression to effectively adapt to environmental adaptations in response to spatial and temporal fluctuations. Histone hyperacetylation has been closely linked to the proliferation, metastasis, and therapeutic resistance of tumor cells. In this investigation, we substantiated the overexpression of the well-documented acetyl-CoA synthetase short-chain family member 2 (ACSS2) at both protein and mRNA levels in breast cancer (BC) cells derived from tumor tissues. Subsequent examinations unveiled that the heightened acetylation of histone H3 in BC cells under environmental stress is contingent upon the accumulation of ACSS2 and enhanced acetyl-CoA synthesis. Intriguingly, the augmentation of H3K9 and H3K27 acetylation (H3K9/K27ac) induced by nutrient stress, mediated by ACSS2, was primarily governed by the histone acetyltransferases (HATs) CBP/p300, with no significant association with conventional histone deacetylases (HDACs). Supplementation with an alternative carbon source, acetate, confirmed that targeted inhibition of ACSS2 mitigated the further elevation of ATP-binding cassette (ABC) transporters, specifically ABC subfamily B member 1 (ABCB1/MDR1) and breast cancer resistance protein (BCRP/ABCG2). These transporters reportedly play crucial roles in both energy metabolic homeostasis and the modulation of intracellular drug concentrations, driven by histone H3 hyperacetylation. Mechanistically, inhibitors of ACSS2 significantly mitigated the resistance of BC cells to doxorubicin and cisplatin, predominantly by reducing H3K27ac levels through the downregulation of nuclear acetyl-CoA content and constraining its binding to the promoters of MDR1 and BCRP. The poor overall survival of BC patients associated with high ACSS2 expression and its positive correlation with MDR1 and BCRP were further confirmed in human BC tumors. Consequently, histone acetylation induced by ACSS2 emerges as a promising epigenetic target for the treatment of BC.

Introduction

As of 2020, breast cancer (BC) represents one of the deadliest cancers, boasting the highest incidence rate and accounting for approximately 30% of female cancer cases. It presents as a heterogeneous tumor with four distinct subtypes: luminal A, luminal B ($HER2^-$/$HER2^+$), HER2-enriched, and triple-negative (TNBC)[1]. Despite the availability of various treatment modalities such as surgery, radiotherapy, endocrine therapy, targeted therapy, and chemotherapy, BC remains a formidable challenge, particularly in individuals at high risk of recurrence and metastasis. Chemotherapy plays a crucial role in the clinical management of BC. However, the accelerated multiplication of cancer cells and the presence of subclinical lesions, coupled with inherent or acquired molecular mechanisms, contribute to drug resistance and diminished treatment efficacy. Consequently, the 5-year survival rate for BC patients remains dismal[2]. In the context of China's sizable population, despite improved awareness and early detection efforts, the incidence of BC continues to rise, especially among younger individuals. Even slight increases in incidence or mortality rates pose significant threats to at-risk individuals and entail a substantial economic burden[3, 4]. It is widely thought that the growth, aggressiveness, and response to

treatment in BC are intricately mediated by bidirectional communication between cancer cells and the surrounding stromal components. This communication occurs through energy and substance loops, facilitating intercellular interactions. The influence of hypoxia, nutrient deprivation, and aerobic glycolysis in recruiting and sustaining drug resistance has been reported across various cancers, including gastric cancer, hepatocellular cancer, and BC [5–8]. Understanding the novel regulatory mechanisms underlying environmental stress could potentially drive advancements in BC treatment. Unraveling these intricate processes may offer new therapeutic targets and strategies to overcome drug resistance, ultimately improving the prognosis for individuals grappling with this formidable disease.

It is widely acknowledged that the deficiencies in vascular structure, distribution, and supply capacity result in most tumor cells experiencing fluctuations in the dynamic supply of oxygen and nutrients, as well as challenges in metabolite clearance during rapid expansion. Over time, tumor cells adapt and accumulate, becoming more aggressive through metabolic reprogramming and susceptibility to malignant progression[2]. Despite this understanding of the tumor microenvironment, the comprehension of therapeutic resistance remains limited, and the intricate mechanisms underlying its formation pose challenges, constraining the development of effective drugs for targeted therapies. In recent decades, substantial efforts have revealed that, beyond genetic mutations, epigenetic alterations in response to environmental stress such as DNA methylation, histone modifications, and changes in non-coding RNAs play pivotal roles in the development of chemoresistance in BC[9]. Notably, histone modifications, particularly histone acetylation, reportedly disrupt the electrostatic affinity between histones and DNA, closely influencing gene transcriptional activity and implicating drug-resistant proteins[10–12]. The processes of histone acetylation are orchestrated by the dynamic activities of histone acetyltransferases (HATs) and histone deacetylases (HDACs), along with the nuclear localization of various metabolic enzymes that facilitate acetyl-CoA production [10]. As mentioned earlier, alterations in lipid metabolism are commonly observed in tumor growth, and short-chain fatty acids (SCFAs) like butyrates or acetate, potent HDAC inhibitors typically derived from gut microbes metabolizing dietary fiber and endogenous recycling, can upregulate ATP-binding cassette (ABC) drug transporters, specifically ABC subfamily B member 1 (ABCB1/MDR1) or breast cancer resistance protein (BCRP/ABCG2). These transporters represent common mechanisms in the development of multidrug resistance (MDR) in BC[2, 13–17]. Collectively, these findings suggest the possibility that targeted intervention in aberrant lipid metabolism in cancer cells could potentially be effective in reversing hyperactivated histone acetylation and consequently mitigating the development of drug resistance in BC.

Acetyl-coenzyme A (acetyl-CoA) synthetase short-chain family member 2 (ACSS2) serves as a metabolic enzyme primarily responsible for converting acetate to acetyl-CoA, thereby maintaining histone acetylation and gene activation crucial for cancer cell growth and survival under environmental stress. Typically located in the cytoplasm, ACSS2 translocates to the nucleus in a stable, phosphorylated form[18–20]. A growing body of evidence highlights the pivotal roles of ACSS2 in ATP production through the tricarboxylic acid cycle, facilitating *de novo* lipid and cholesterol biosynthesis, promoting acetate utilization, and stabilizing lipid biomass to support tumor growth[18–22]. Moreover, the abundance of ACSS2 exhibits variations with tumor progression and various environmental changes,

including glucose deprivation, hypoxia, acidic pH, and nutrient starvation conditions [19, 20, 23–25]. While the influence of ACSS2 levels on cancer progression remains controversial to some extent, clinical data predominantly associate its upregulation with poor prognosis in multiple cancer patients[26–30]. In BC, ACSS2 levels have been reported to be lower than in mammary fibroma tissues. Notably, ACSS2 overexpression has been shown to mitigate the effects of cadmium exposure, a known risk factor for BC, by inducing proliferation, migration, and invasion[31, 32]. In diverse studies, ACSS2 upregulation has been linked to increased acetyl-CoA levels and enhanced autophagy, promoting survival in estrogen-deprived and tamoxifen-treated BC cells and facilitating cell growth under hypoxic and nutrient-depleted conditions. High expression of ACSS2 in TNBC has been associated with shorter overall survival compared to negative cases[33–35]. Our previous research has demonstrated that nutrient stress-induced ACSS2 accumulation contributes to cisplatin resistance in esophageal squamous carcinoma cells (ESCCs)[36]. However, the expression and roles of ACSS2 in BC, including its regulatory mechanisms and impact on progression, warrant further investigation. Herein, we sought to investigate whether inhibiting ACSS2 could attenuate the development of chemoresistance induced by microenvironmental stress. Our findings revealed that ACSS2 exhibited sustained and stable levels of acetyl-CoA during supply shortages, leading to intense histone acetylation and subsequent synthesis of abundant ATP-binding cassette drug transporters in BC.

Materials and methods

Human sample

The study protocol and informed consent forms were obtained from all the participants and the tenets of the Declaration of Helsinki were followed. A total of 113 BC patients aged 50 ~ 67 years who underwent adenomammectomy in the Affiliated Hospital of Jiangsu University were recruited for this study.

Reagents and antibodies

ACSS2 inhibitor (#S8588) and another inhibitor targeting ACSS2 (VY-3-135, #E1147), Trichostatin A (TSA, #S1045), A-485 (#S8740), Cisplatin (DDP, # S1166), Doxorubicin HCl (Dox, #S1208) were purchased from Selleck Ltd. (Shanghai, China). Reagents for cell culture, penicillin/streptomycin (100×), Dulbecco's modified Eagle's medium (DMEM, 4.5g/L D-glucose), RPMI 1640, Leibovitz's L-15 and Minimum essential medium (MEM) were from Gibco (Thermo Fisher Scientific, USA). DMEM (1.0 g/L D-glucose) was from Procell Life Science & Technology Co., Ltd. (Wuhan, China). Sodium pyruvate, L-alanyl-L-glutamine, and recombinant human insulin were obtained from Zhong Qiao Xin Zhou Biotechnology Co., Ltd. (Shanghai, China). Fetal bovine serum (FBS) was purchased from Biological Industries Ltd. (Kibbutz Beit Haemek, Israel). Acetyl-CoA was obtained from Solarbio Technology Co., Ltd (Beijing, China). Acetate and RIPA lysis buffer were purchased from Sigma-Aldrich (Missouri, USA). Antibodies against ACSS2 and ACSS2 (Phospho-Ser659) were obtained from Abcam (#ab66038, Boston, USA) and Signalway Biotechnology (#58003, Pearland, USA), respectively. Antibodies specific for CBP, p300, PCAF, GCN5L2, MDR1, HDAC3, HDAC4, HDAC5, HDAC8, Acetyl-Histone and Acetyl-Histone H3 antibody sampler kit, and cleaved caspase-

3 were purchased from Cell Signaling Technology (Danvers, USA). Antibodies against ACSS1, ACSS3, Bax, BCRP, Lamin B1, α-Tublin, GAPDH, anti-rabbit and anti-mouse IgG-conjugated horseradish peroxidase (HRP) was purchased from Proteintech Group (Wuhan, China). Tumor dissociation kit (human, #130-095-929) and the supporting equipments were obtained from Miltenyi Biotechnology. The siRNA transfection reagent RFect was purchased from Bio-generating Biotechnology (Changzhou, China). The VeZol Reagent, DNA transfection reagent ExFect, BCA (bicinchoninic acid) protein assay kit, enhanced chemiluminescence (ECL) kit, protein marker, CCK-8 cell counting kit, HiScript III RT SuperMix and ChamQ SYBR® qPCR master mix were obtained from Vazyme Biotechnology Co., Ltd. (Nanjing, China). Acetyl coenzyme A ELISA kit, primers, small interfering RNAs (siRNAs) targeting ACSS2, CBP, p300, PCAF, GCN5, MDR1, BCRP and negative control siRNA were purchased from Sangon Biotech Co., Ltd. (Shanghai, China).

Immunohistochemistry (IHC) analyses

IHC was performed according to the standard protocol. Briefly, the tissue sections were deparaffinized by xylene, retrieved by boiling sodium citrate, blocked with 10% goat serum, and incubated with primary antibody overnight at 4°C. The following primary antibodies used were antibodies against ACSS2 (1:800), MDR1 (1:500), BCRP (1:800). The quantification of expression was evaluated by two independent pathologists. Both sets of results were combined to give a mean score for further comparative evaluations. The IHC score was determined by combining the percentage and the staining intensity of positively stained tumor cells as the previous article[36]. Such method was used to evaluate ACSS2 expression in BC and adjacent normal samples. We use the median value as the cut-off to define high and low in BC samples for ACSS2 expression analysis and that in all patients in chemotherapy evaluation.

BC cell culture and drug treatment

Human BC cells, MCF-7, T-47D, MDA-MB-231 and MDA-MB-468, were purchased from Zhong Qiao Xin Zhou Biotechnology Co., Ltd. (Shanghai, China) and obtained from the American Type Culture Collection (ATCC, Rockville, USA). T-47D cells were cultured in DMEM, MDA-MB-231 and MDA-MB-468 cells were maintained in L-15 medium, MCF-7 cells were gown in MEM containing with 1% L-alanyl-L-glutamine and 0.01%human recombinant insulin. All cell lines were supplemented with 10% FBS and 1% penicillin/streptomycin, passaged at 80% confluency and tested negative for pathogens, including mycoplasma. T-47D and MCF-7 cells were cultured in a humidified incubator of 5% CO_2 at 37°C, while MDA-MB-231 and MDA-MB-468 cells were maintained in 100% air, respectively. For additional experiments, The concentration of FBS in the cell culture medium was reduced from 10–1% for more than 48 h as a nutrient stress treatment, and the supplemental carbon source was added by addition of acetate (0.5 mM) to simulate exogenous addition, and the hypoxic condition was achieved by using a triple gas incubator, controlling the oxygen concentration at 1% for 7 days. Expression of ACSS2, acetyl-CoA, H3K9 and H3K27 in BC cells were documented following treatment with the ACSS2 inhibitors (5 μM), or VY-3-135 (50 nM), CBP/p300 inhibitor A-485 (5 μM) and the TSA (0.5, 1.0 and 2.0 nM). To determine the sensitivity or resistance to chemotherapeutic drugs, BC cells were exposed to Dox (1.0, 2.0,

4.0, 8.0, 16.0, 32.0, 64.0, 128.0 and 256.0 nM or 5nM) and DDP (5 mM) according to different experimental purposes.

Western blotting and RT-qPCR analysis

The protein levels of specified proteins in tumors, normal tissues, and BC cells were determined through Western blotting. In brief, breast tissue and cell samples were lysed in RIPA lysis buffer containing PMSF and protease inhibitors in appropriate proportions. The protein concentrations of lysates were quantified using a BCA protein assay kit. Equal amounts of proteins were separated by SDS-PAGE (sodium dodecyl sulfate-polyacrylamide gelelectrophoresis) and transferred to PVDF (polyvinylidene fluoride) membranes (Merck Millipore, Billerica, MA, USA). The membranes were blocked in 5% nonfat milk dissolved in TBST for 60 minutes, followed by overnight incubation with primary antibodies at 4°C. After washing, the membranes were incubated with HRP-conjugated secondary antibodies for an additional 60 minutes at room temperature. Following three washes with TBST, the membranes were analyzed using a gel imaging system (Tanon Science & Technology Co. Ltd., Shanghai, China) with ECL reagent. For the assessment of mRNA levels of ACSS1, ACSS2, ACSS3, MDR1 and BCRP in cells, qPCR was employed based on our previous methodology[36]. Total mRNA was extracted using VeZol reagent, and cDNA synthesis was carried out using HiScript III RT SuperMix. qPCR was performed on QuantStudio™ 5 DX (Thermo Fisher Scientific, Waltham, MA, USA) using ChamQ SYBR® qPCR master mix. Primers used for targeted genes were ACSS1, 5'-TGGCAAGATCGGCTGGTTCC-3' (forward) and 5'-TCACTTCCGTTCCAGGCTCATC-3' (reverse); ACSS2, 5'-GCACGGCAGACATTGGTTGG-3' (forward) and 5'-TGCTCCACAGGCGGTTCAC-3' (reverse); ACSS3, 5'-CGTGACCTTGATTGGGATGAAGAG-3' (forward) and 5'-CGTTGTGCCAGATGTGTAAAGAATATAC-3' (reverse); MDR1, 5'- ACTATTGTTTCTAGCCCTTGGAATTATTTC-3' (forward) and 5'- ATCGGAGCCGCTTGGTGAG-3' (reverse); BCRP, 5'- TCGTACTGGGACTGGTTATAGGTG-3' (forward) and 5'-GTTGGTCGTCAGGAAGAAGAGAAC-3' (reverse); GAPDH, 5'-ACAGCCTCAAGATCATCAGCAA-3' (forward) and 5'-ACCACTGACACGTTGGCAGT-3' (reverse). RNA expression levels of the targeted genes were determined using the $2^{-\Delta\Delta CT}$ method, normalized to the expression of GAPDH.

Preparation of single-cell suspensions from resected samples

Fourteen pairs of primary BC tumors and corresponding normal breast tissues were separately collected and processed, with each step limited to a 1 h duration, utilizing the Miltenyi tissue dissociation kit. Briefly, the tissues were rinsed with cold PBS to eliminate blood and surface attachments, and then cut into small cubes with an edge length of approximately 1 mm. These tissue fragments were subjected to a digestion buffer containing an enzyme mix, followed by 30 min incubation and grinding at 37℃ on the Miltenyi Gentle MACS, as per the manufacturer's instructions. Subsequently, the resulting cell suspension underwent filtration through a 70 μm filter and was centrifuged for 10 min at 350 g, 4℃. Following the removal of any remaining erythrocytes or dead cells using an ammonium chloride solution, the remaining cells were ultimately resuspended in RIPA lysis buffer or VeZol reagent, ready for subsequent Western blotting and RT-PCR analyses.

RNA interference, plasmids, and lentiviral construction

Small interfering RNA (siRNA) and plasmid transfections were conducted using RFect and DNA transfection reagent ExFect, respectively. The siRNA sequences targeting ACSS2, CBP, p300, GCN5, PCAF, MDR1, BCRP, and the negative control group are listed in Supplemental Table 1. The plasmids of ACSS2 (NM_018677.4), MDR1 (NM_001348946) and BCRP (NM_004827) were purchased from MiaoLing Biotechnology Co., Ltd (Wuhan, China), and they were transfected into BC cells following the manufacturer's instructions. The efficiency of overexpression was assessed by Western blotting 48 hours after transfection. For shRNA-ACSS2 sequence was selected from siRNA-ACSS2 (#1). Lentiviruses carrying shRNA-ACSS2 and control sequences (GeneChem Technology, Shanghai, China) were transfected into MDA-MB-468 cells according to the manufacturers' instructions. Subsequently, the transduced cells were treated with puromycin (2 μg/mL) to establish stable ACSS2 knockdown cell lines.

Cell fractionation assays

Cytoplasmic and nuclear fractionations were carried out using an extraction kit (Beyotime Institute of Biotechnology, Shanghai, China) following the manufacturer's protocol. In brief, a total of 1×10^7 cells were scraped and resuspended in 500 μL of hypotonic buffer. After vortexing, incubation, and centrifugation (12000g, 5 min) at 4°C, the resulting supernatant was collected as the cytoplasmic fraction. For the pellet, after thoroughly removing the remaining supernatant, it was resuspended in 100 μL hypertonic buffer containing PMSF. Subsequently, the mixture was vortexed, treated in an ice bath, repeated for 30 min, and finally centrifuged (12000g, 10 min) at 4°C. The resulting supernatant was considered the nuclear fraction.

Detection of acetyl-CoA

Cellular acetyl-CoA levels were determined using an ELISA kit following the manufacturer's protocol. In brief, cells were gently washed with a moderate amount of pre-cooled PBS and then dissociated using trypsin. After centrifugation (1000g, 5 min) at 4°C, the cells were washed three times with cold PBS. For every 1×10^6 cells, 200 μL of PBS was added to maintain cell suspension. The cells underwent several freeze-thaw cycles until fully lysed, followed by centrifugation for 10 minutes at 1500g and 4°C. To generate an acetyl-CoA standard curve, various concentrations (20, 10, 5, 2.5, 1.25, 0.63, 0.31, 0 ng/mL) of the acetyl-CoA standard provided were used. The concentration was calculated using the Multiskan GO™ microplate reader (Thermo Fisher Scientific, Waltham, MA, USA) at 450 nm.

Cell Counting Kit-8 assays

Cell viability and half maximal inhibitory concentration (IC_{50}) value were evaluated by Cell Counting Kit-8 (CCK-8) assay according to the manufacturer's instructions. Cells (2×10^3 cells per well) were plated in 96-well plates in triplicate. CCK-8 was added to each well at a final concentration of 10% at different time points, and incubation continued at 37°C for 20 to 30 min. Then, the absorbance of the samples was measured at 450 nm using the microplate reader to calculate the numbers of viable cells in each well.

Apoptosis assays

To analyze cell apoptosis, 5×10^4 cells were harvested, washed, resuspended and stained with Annexin V/7-AAD apoptosis detection kit according to the manufacturer's instruction. The Annexin V positive cells were regarded as apoptotic cells, while negative for both Annexin V and 7-AAD were defined as viable ones. Flow cytometry analysis was carried out with BD FACS Canto™ II flow cytometer (BD Biosciences, San Jose, CA, USA), and acquired data were analyzed using FlowJo™ software (Version 10.8.1, Oregon, USA).

Chromatin Immunoprecipitation (ChIP)

The ChIP assay was conducted following the kit (Beyotime Institute of Biotechnology, Shanghai, China) instructions. A total of 1×10^7 cells were collected and crosslinked in a 1% formaldehyde solution for 10 min at 37°C, followed by the addition of 1.1 mL Glycine Solution (10×) for 5 min at room temperature. The extract was sonicated using Fisherbrand™ Sonic Dismembrator (Thermo Fisher Scientific, Waltham, MA, USA), followed by centrifugation, and immunoprecipitation was performed with an H3K27ac antibody, with normal IgG used as the negative control. The immunoprecipitated samples were eluted and reverse crosslinked, after which the DNA fragments were purified. Immunoprecipitated and input DNAs were then subjected to RT-qPCR analysis, and primer sets targeting the MDR1 and BCRP promoters were designed and are listed in Supplemental Table 2.

Statistical analysis

All results were confirmed in at least three independent experiments, and data from one representative experiment were shown. All quantitative data are presented as means ± SD. For those datasets that fulfilled Pearson normality test criteria, an unpaired Student's t test was performed. Moreover, nonparametric Mann-Whitney test was chosen. Fisher's exact test or chi-square test was used for the analyses of contingency tables depending on the sample sizes. Kaplan-Meier method was used to estimate the survival rate, and the difference between survival curves of two groups was assessed by the log-rank test. Statistical significance was considered at the level of $P < 0.05$.

RESULTS

The upregulation of ACSS2 in BC responses to microenvironmental variation

While previous research has illuminated the roles of ACSS family members in various cellular processes such as metabolism, survival, growth, migration, and invasion, their specific functions in the context of therapy resistance in BC remain poorly understood[21, 31–35, 37–40]. To identify gene expression differences between breast tumors and normal tissues, we initially investigated the levels of ACSS1, ACSS2 and ACSS3 in TCGA (The Cancer Genome Atlas)-BRCA, utilizing data from the TCGA data portal. Analysis based on the expression data of 1126 tumors and 113 normal tissues indicated a significant

decrease in the expression of ACSS2 and ACSS3 in human BC compared to normal tissues. Interestingly, ACSS1 expression displayed a large fluctuation but showed a more significant increase (Supplementary Fig. 1A). Consistent with these findings, paired samples demonstrated a similar trend among ACSS family members in individuals with BC (n = 113; Supplementary Fig. 1B). In contrast to earlier studies, where genetic or epigenetic alterations might influence BC progression in ACSS expression driven by the tumor microenvironment, our results suggested a clear difference among ACSS family members at the transcriptional level. Particularly noteworthy was the apparent contradiction between the expression pattern of ACSS2 and its function[21, 31–35]. Consequently, we sought to study their expression in single-cell suspensions derived from fresh tumors and adjacent normal tissues. Interestingly, ACSS2 mRNA expression was significantly increased in breast tumors, while ACSS1 and ACSS3 expression did not show significant elevation overall, with no marked difference between normal samples and paired tumors (Fig. 1A). Further examination of cells harvested from human tissues revealed an even more pronounced distinction in ACSS2 expression between tumors and adjacent normal tissues (Fig. 1B). This observation aligned with the transcriptional results, indicating that the protein levels of ACSS1 and ACSS3 are not only unstable but also challenging to discern through Western blotting, whether in tumors or normal tissues from BC patients. Given the association of high ACSS2 expression with shorter overall survival and escalating tumor stage, particularly in TNBC sections, we randomly selected and compared 47 paired breast tumors and normal tissues to further validate ACSS2 expression[34, 35, 41, 42]. Despite the relatively weak and sporadic distribution of some epithelial cells in the basal layer and endothelial cells, ACSS2 exhibited more insignificant effects on the stabilization, function, and metabolic activity of normal breast tissues compared to tumors. ACSS2 was predominantly localized in the cytoplasm of cancer cells at the edge of clusters, accompanied by invasive processes. This was in contrast to its rare nuclear distribution in the core of densely packed cell regions (Fig. 1C). These results suggest that the majority of ACSS2 in tumors primarily arises from the accumulation of cancer cells and indicate a strong association with malignant behaviors.

To assess the functional implications of ACSS family members, we examined the basal and post-stimulation dynamics of their expression across various BC cell lines, including MCF-7, T-47D, MDA-MB-231, and MDA-MB-468, rather than focusing solely on TNBC[21, 31, 34, 38]. Western blotting revealed that among all the members of the ACSS family, ACSS2 exhibited the most significant upregulation in the MDA-MB-468 cell line compared to MCF-7, T-47D, and MDA-MB-231 cell lines. Conversely, ACSS1 and ACSS3 showed higher abundance in MCF-7 cells, while ACSS1 and ACSS3 were absent in MDA-MB-468 cells, and overall, the expression of ACSS1 and ACSS3 was comparable among BC cells (Fig. 1D). Metabolic changes often accompany tumor progression, and microenvironmental variations may precede genetic alterations in cancer cells. Increased ACSS2 expression was also observed in T-47D cells following acetate addition and nutrient starvation, with the latter being a classical stimulus that enhances ACSS2 expression and activity[34]. As a conserved metabolic enzyme involved in both fatty acid and cholesterol biosynthesis, ACSS2 slightly accumulated under low glucose conditions or when exposed to hypoxia in T-47D cells. Moreover, the extent of ACSS2 expression significantly varied after nutrient starvation in MCF-7 and MDA-MB-468 cell lines, while no significant changes in ACSS1 and ACSS3 were

observed simultaneously (Fig. 1E and Supplementary Fig. 1C). This suggests a positive correlation between ACSS2 levels and malignant characteristics, particularly under microenvironmental stress in BC cells.

Effects of ACSS2 on the acetyl-CoA levels and histones acetylation in BC cells

To identify effective treatment strategies for patients with initially high ACSS2 expression or increased expression with disease progression, we sought to explore the molecular mechanisms that drive BC malignancy. Given that the presence of ACSS2 has been demonstrated to induce acetyl-CoA accumulation in human breast ductal cancer and prostate cancer cell lines, we investigated acetyl-CoA levels in BC cell lines using chemical inhibitors or RNA interference targeting ACSS2[34]. Indeed, both the MCF-7 and MDA-MB-468 cell lines exhibited higher acetyl-CoA levels compared to other cell lines. Furthermore, treatments with siRNA-ACSS2 led to a reduction in acetyl-CoA levels, with effective suppression achieved at 24 hours. The extent of suppression was negatively correlated with the duration of interference. The intensity of acetyl-CoA in MDA-MB-468 cells with ACSS2 knockdown decreased to approximately 28% of that in the negative control cells, while the reduction reached 54% in MCF-7 cells over 48 hours. Conversely, when ACSS2 was overexpressed, there was a significant increase in acetyl-CoA synthesis in T-47D cells (Fig. 2A, 2B and Supplementary Fig. 2A, B), suggesting that the availability of ACSS2 protein influenced the basal acetyl-CoA levels in these cell lines. In summary, inhibiting ACSS2 in the complex and variable tumor microenvironment yields a significant change in energy metabolism and gene expression, primarily due to the reduced levels of acetyl-CoA.

Previous studies have demonstrated that hyperactivated ACSS2 sustains high concentrations of nuclear-cytosolic acetyl-CoA, supporting acetylation, fatty acid synthesis, and cell growth in multiple cancers[18, 22, 43–46]. Recent research on BC has highlighted the distinct function and role of ACSS2 in tumor metabolism, particularly acetate consumption. Moreover, ACSS2 overexpression has been shown to increase H3K27 acetylation levels to maintain autophagy[21, 32–35, 38]. However, a comprehensive understanding of how ACSS2 contributes to histone acetylation in BC warrants further investigation. Given that a sufficient number of acetyl-CoA molecules are crucial for protein acetylation, this study aimed to investigate the broad impact of ACSS2 on histone acetylation in BC. Nutrient starvation induces significant changes in lipid metabolism, creating a dependence on *de novo* lipogenesis for survival under metabolic stress, which can be restored through ACSS2-mediated acetyl-CoA synthesis.[34, 35]. In MCF-7 and MDA-MB-468 cells, loss of ACSS2 resulted in defects in the induction of H3K9 acetylation in response to constant nutrient stress (Fig. 2C). Even under normal growth conditions, BC cells treated with ACSS2 inhibitors harbored lower levels of H3K9ac and H3K27ac proteins than untreated groups, suggesting that ACSS2 downregulation or inactivation impairs histone H3 acetylation. This effect was more pronounced under nutrient starvation, where enhanced H3K9ac and H3K27ac levels were significantly reversed, and these two proteins were positively correlated with acetyl-CoA levels (Fig. 2D and Supplementary Fig. 2C). These findings indicate that ACSS2 maintains abundant levels of acetyl-CoA in BC cells, ensuring an adequate substrate for protein acetylation under microenvironmental stress.

Protein acetylation involves a family of enzymes known as acetyltransferases, including CBP, p300, PCAF, and GCN5. Western blot analysis revealed a normal baseline of H3K9ac and H3K27ac with the silencing of CBP and p300. No significant differences in the expressions of these acetyltransferases were observed both before and after exposure to 1% serum conditions (Fig. 2E). Furthermore, concerning the deacetylases, represented by HDAC3, HDAC4, HDAC5, and HDAC8, their expressions displayed variations without reaching statistical significance, indicating homogeneous differences. Further exploration revealed that targeted interference of CBP completely blocked ACSS2-mediated enhancement of H3K9ac expression in T-47D cells (Supplementary Fig. 2D and 2E). However, supplementation of acetyl-CoA was not able to reverse the retraction of histone H3 acetylation caused by ACSS2 inhibition (Fig. 2F). Consistent with previous studies, BC cells exhibited higher acetyl-CoA and H3K9/K27ac protein levels under nutrient stress plus acetate supplementation (Fig. 2F and Supplementary Fig. 2F)[19]. The inhibition of ACSS2 or its nuclear translocation suppressed the increase in histone acetylation, indicating that ACSS2 is sufficient to provide a steady stream of acetyl-CoA under stress and consequently increase histone H3 acetylation in BC cells.

Effects of ACSS2 on the expression of efflux transporters of BC cells

Efflux transporters, primarily referring to ABC transporters, play a crucial role in the formation of physiological barriers such as the blood-brain barrier, intestine, liver, and kidney, impacting the pharmacokinetic properties of various drugs and metabolites, including SCFAs[13, 47, 48]. Acetate, as a key member of SCFAs, has been shown to significantly decrease MDR1 while increasing BCRP protein expression in rat intestines, mouse intestinal epithelial cells, and human colorectal adenocarcinoma cells[13]. Given this, the study hypothesized that the overlapped H3 acetylation observed under nutrient starvation might be partly due to acetate-induced changes in MDR1 and BCRP. To validate this hypothesis, the present study compared MDR1 and BCRP levels under nutrient stress with the addition of acetate or a combination of both. Additionally, the present study examined whether modulation of efflux transporter expression affected intracellular ACSS2 and H3 acetylation levels. The results showed no significant difference in the expression of MDR1 with additional acetate treatment alone, while a significant increase in MDR1 and BCRP was observed under nutrient stress. Interestingly, the reduction of MDR1 and BCRP did not alter the expression of ACSS2 levels but efficiently blocked the acetylation of histone H3, both in the presence of acetate alone and in combination with low serum (Fig. 3A and Supplementary Fig. 3A). This indicates that the responses of efflux transporters may be an essential driver of metabolic reprogramming in response to the threats of the tumor microenvironment. The present study then investigated whether the increased levels of MDR1 and BCRP under nutrient stress depended on the presence of ACSS2 protein involved in gene regulation[14, 15]. The initially upregulated levels of MDR1 and BCRP were observed to return to pre-stimulus levels after siRNA-ACSS2 treatment at 24 hours. Furthermore, the overexpression of ACSS2 in T-47D cells enhanced the fundamental levels of MDR1 and BCRP, suggesting that ACSS2 activation driven by nutrient shortage was directly involved in the regulation of acetate transportation in BC cells (Fig. 3B and Supplementary Fig. 3B). We also explored whether modulating ACSS2 activation affects the mRNA levels of MDR1 and BCRP in MDA-MB-468 cells. MDR1

and BCRP were significantly increased by 3.16- and 2.69-fold under nutrient stress at 24 hours, but these increases were effectively blocked by pretreatment with the ACSS2 inhibitor. Moreover, the consistent elevation of MDR1 and BCRP levels was observed in response to conditions of nutrient starvation (Fig. 3C).

To investigate the impact of histone acetylation on transporter expression regulated by ACSS2, the present study employed A-485 to inhibit CBP/p300 activity. A-485 is a selective acetyltransferase inhibitor of CBP/p300 that binds in the enzymes' active site as an acetyl-CoA competitor[49]. In agreement with the roles of ACSS2 in the regulation of acetyl-CoA expression, A-485 treatment led to a decrease in H3K27ac, with concurrent overexpression of ACSS2 resulting in a blunted upregulation of MDR1 and BCRP (Fig. 3D). Similarly, cells treated with the HDAC inhibitor TSA exhibited a significant increase in the expression of MDR1 and BCRP under ACSS2 knockdown, showing concentration-dependent inductions of the targeted proteins (Fig. 3E). These findings suggest that ACSS2 alone is sufficient to drive H3K27 acetylation, leading to the subsequent increase in the expression of MDR1 and BCRP. To further substantiate these findings, we conducted ChIP assays to investigate whether increased acetyltransferase activity modulates chromatin acetylation at the promoters of MDR1 and BCRP. Using an antibody against H3K27ac, followed by RT-PCR reactions with specific primers, we observed a significant increase in H3K27ac at both regions of the MDR1 and BCRP promoters in cells subjected to nutrient starvation, compared to control cells (Fig. 3F). Overall, our data indicate that BC cells maintain elevated levels of efflux transporters through the activation of H3 acetylation facilitated by enhanced ACSS2 under environmental stress.

ACSS2 inhibition sensitizes BC cells to drugs while its upregulation predicts poor prognosis

In light of the observed alterations in tumor metabolism under environmental stress and considering that MDR1 and BCRP are common pumps involved in multidrug resistance, the study investigated whether ACSS2 could influence the efficacy of MDR1 and BCRP in regulating chemosensitivity. Gene set enrichment analysis (GSEA) revealed a negative correlation between ACSS2 levels and HDACs responsible for histone deacetylation, with a concurrent positive association with fatty acid biosynthesis and ABC transporters involved in lipid homeostasis (Fig. 4A and Supplementary Fig. 4A). To assess ACSS2's involvement in the regulation of drug resistance mediated by MDR1 and BCRP, cells were treated with Doxorubicin (Dox) or Cisplatin (DDP), which are common drugs used in BC chemotherapy. The results demonstrated that Dox or DDP treatment led to an upregulation of apoptosis protein levels in BC cells, an effect mitigated by ACSS2 overexpression and augmented by ACSS2 depletion. Notably, the resistance induced by ACSS2 enhancement was partially reversed by inhibiting MDR1 or BCRP in T-47D cells (Fig. 4B and Supplementary Fig. 4B). These findings indicated that ACSS2 could preserve the expression of efflux transporters in response to the cell-killing effects of drugs. To further assess the impact of ACSS2 on chemosensitivity, cell viability assays were conducted to determine the half-maximal inhibitory concentration (IC_{50}) value. Consistent with the altered expressions and functions of MDR1 and BCRP, the IC_{50} values of Dox in T-47D cells with ACSS2 overexpression were significantly higher at 13.86

± 0.42 nM compared to 8.23 ± 0.33 nM in control cells. Additional results confirmed that, compared with control cells (IC_{50} = 8.67 ± 0.33 nM for Dox), shRNA-ACSS2 significantly decreased the viability of MDA-MB-468 cells exposed to Dox to 75% (Fig. 4C). Furthermore, ACSS2 overexpression exhibited a significant decrease in the apoptosis rate after 48 hours of exposure to Dox compared to control cells. Conversely, the inhibition of MDR1 or BCRP reversed the antiapoptotic effect of ACSS2 overexpression. In line with previous data, the knockdown of ACSS2 markedly increased the rate of apoptotic cells stimulated by Dox, an effect rescued by restoring MDR1 or BCRP expression (Fig. 4D). These findings suggested that ACSS2 desensitizes BC cells to chemotherapeutics by promoting the expression of efflux transporters.

DNA-damaging agents such as Dox and DDP, often employed in combination with other anticancer drugs, are commonly used for the treatment of advanced BC. To assess the clinical significance of alterations in MDR1 and BCRP induced by ACSS2, the correlation between ACSS2 expression and prognosis was examined in BC patients post-chemotherapy. Given that ACSS2 can enhance BC cell resistance to Dox and DDP, an investigation into the association between ACSS2 expression and chemotherapy outcomes was conducted. The study involved the analysis of ACSS2 levels in 48 primary tumor specimens obtained from patients who underwent surgery and received chemotherapy. Remarkably, patients with lower ACSS2 expression exhibited significantly longer overall survival (OS) (Fig. 4E). This observation led to the hypothesis that activated ACSS2 may contribute to the expression of MDR1 and BCRP. To explore this potential association, the relationship between ACSS2 expression and MDR1, as well as BCRP, was examined in BC through immunohistochemistry scoring. The results revealed that malignant cells in breast tumors exhibited a higher rate of MDR1 positivity, close to 60%, compared to about 30% for BCRP-positive cells (Fig. 4F). Elevated ACSS2 expression in breast tumors was concomitant with increased levels of MDR1 and BCRP, further supporting the hypothesis (Fig. 4G). In summary, these findings suggest that ACSS2 reduces the susceptibility of BC cells to Dox and DDP and may serve as a potential predictor of comprehensive treatment outcomes, including chemotherapy responses.

DISCUSSION

Whether in normal or aberrant cells, acetyl-CoA is believed to face a barrier in crossing organelle membranes. It is synthesized and consumed relatively independently across distinct cellular regions, with its stored pool dependent on the expression and activation levels of synthetases. Acetyl-CoA typically exhibits dynamic fluctuations in its abundance and concentration. It can be categorized into nuclear, cytoplasmic, and mitochondrial forms based on its location[50]. There is now widespread recognition that alterations in the overall intracellular level of acetyl-CoA can impact the acetylation process of proteins, including histones. Enzymes capable of generating acetyl-CoA in the nucleus play a crucial role, broadly or site-specifically regulating histone acetylation to influence the expression of targeted genes responsive to internal and external stimuli[19, 34, 35, 50]. ACSS2 is a key focus of diverse studies and has been acknowledged as a critical synthetase. It can directly utilize acetate and recycle it through deacetylation reactions, distinguishing it from other members (ACSS1 and ACSS3)[19, 23, 34, 35, 50]. Moreover, it is well-established that the molecular mechanisms involved in modulating ACSS2 production

and upregulating its expression vary significantly in response to specific stimuli across different cell types and even within the same cell. For example, in caprine mammary epithelial cells and mouse liver cells, ACSS2 is implicated in the synthesis of fatty acids and sterols from free acetic acid. Its regulation is directly influenced by sterol regulatory element-binding protein 1 (SREBP-1), a nuclear transcription factor recognized as essential in lipid anabolism[51, 52]. In other organisms, such as chickens, the gut microbiota plays a regulatory role in adipogenesis. Dysregulation of the gut flora induced by a high-fat diet can lead to a significant reduction in the abundance of butyric acid. This reduction, in turn, inhibits miRNA-204 in the liver, resulting in the up-regulation of ACSS2, a downstream target gene negatively regulated by miRNA-204. Ultimately, this molecular cascade contributes to the development of obesity[53]. In bovine adipocytes, miRNA-193b has been identified as a regulator that downregulates the expression of ACSS2. This downregulation inhibits cell proliferation and differentiation while promoting apoptosis[54]. In human vascular smooth muscle cells, a different non-coding RNA, miRNA-15b-5p, plays a role in blocking cell proliferation. This is achieved by inhibiting the expression of ACSS2 and inducing apoptosis [55]. In contrast to cells in normal tissues, tumor cells within tumors exhibit unrestrained growth, dysregulated differentiation, and senescence resistance, necessitating adaptation to fluctuations in nutrient, carbon source, and oxygen supply in their environment. While the expression level and role of ACSS2 in tumor progression, including BC cells, remain controversial, there is consensus that lipid metabolism involving ACSS2 and its synthesis of acetyl-CoA directly impacts the survival and invasion of tumor cells[18–20, 26–30]. Studies on breast ductal carcinoma cells have revealed that increased ACSS2 expression, triggered by insufficient oxygen supply, is regulated by the combined action of SREBP2 and HIF. In hepatocellular carcinoma cells under hypoxic conditions, acetate supplementation elevates mRNA levels of both ACSS1 and ACSS2. This elevation may be linked to enhanced binding of acetylated histone proteins, such as H3K9ac and H3K27ac, to their promoters. ACSS1 and ACSS2 are reportedly implicated in facilitating histone H3 acetylation, forming a positive loop in response to environmental stress[34, 56]. Despite the varied performances of ACSS family members in BC studies, bioinformatics analysis revealed significantly higher transcriptional levels of ACSS1 in BC tissues compared to others. Recognizing the diversity in cell populations within breast tissues, our study provided hitherto undocumented evidence through single-cell suspensions that both transcriptional and protein expression levels of ACSS2 were notably higher than those of ACSS1 and ACSS3, which were mostly undetectable in normal tissues. IHC further confirmed elevated ACSS2 expression in tumor cells, primarily in areas of high density and infiltration structures, suggesting a strong association between heightened ACSS2 expression and aggressive progression in BC. Exploring its precise molecular function, especially in acetyl-CoA modulation, holds promise for more targeted therapeutic interventions in the future.

The acetyl-CoA generated and supplied by ACSSs serves as a critical intermediate in various metabolic pathways within numerous tumors, acting as a foundational material for substance synthesis. Additionally, it plays a crucial role in epigenetic modification through protein acetylation, providing acetyl substrates. To explore the contextual factors influencing differences among ACSS family proteins in breast tumors and elucidate the unique role of ACSS2 in BC malignancy, we simulated the tumor microenvironment based on our prior research and integrated findings from other studies. We constructed

in vitro treatments mimicking common environmental stresses such as glucose deprivation, nutrient stress, and hypoxia[25, 34, 36, 56]. Consistent with numerous studies, particularly those involving TNBC cells, our results indicate that ACSS2 was markedly more sensitive and responsive than other ACSS family members when faced with metabolic stress. However, a comprehensive analysis of all changes revealed that, in the context of hypoxia and glucose deprivation, ACSS1 and ACSS3, which were inherently present at low levels, did not exhibit a unified, effectively upregulated, and continuously replenished response. Furthermore, the stimulatory effect of nutrient stress on ACSS1 and ACSS3 was found to be extremely limited[34, 35]. It is highly conceivable that the observed increase in ACSS2 under nutrient stress is linked to heightened malignant behaviors in BC. This prediction is crucial for unraveling the role of microenvironmental stresses in the metabolic reprogramming process. Furthermore, we demonstrated that the continuous expansion and replenishment of intracellular acetyl-CoA storage in BC cells during nutrient limitations primarily relies on the stable expression and increase of ACSS2. Given that the accumulation of ACSS2 is associated with enhanced acetate recycling and utilization, tightly correlated with malignancy indicators like tumor cell growth and metastasis, we hypothesized that this process in BC cells could result in increased utilization of acetyl-CoA for energy supply, molecular biosynthesis, and protein acetylation, including histones in particular[20–25]. However, we acknowledge that histone acetylation modification involves precise spatiotemporal regulation of related enzymes, as previously described. Any alterations in this part of the process may depend on two scenarios[50]. The depletion of acetate caused by increased ACSS2, or the resulting acetyl-CoA acting as a lipid synthesis intermediate, may lead to alterations in the levels of other SCFAs, thereby implicating SCFAs as broad-spectrum inhibitors of histone deacetylases. It is also plausible that the heightened intensity of ACSS2 and the robust level of acetyl-CoA could potentially impact the expression and activity of histone acetyltransferases. In this respect, studies have demonstrated that ACSS2 enhances the activity of HATs such as CBP and PCAF. In other words, the metabolic reprogramming induced by environmental stress, utilizing acetate as an alternative carbon source for tumor cells, may be dependent on epigenetic modifications. The main focus of our study was on histone acetylation, as it plays a profound and meaningful role in adapting to changes. Our study revealed consistent enhancement of histone H3 acetylation in BC cells with high ACSS2 expression compared to other histones. ACSS2 is identified as a driver initiating gene expression and synthesis in BC cells, while HATs and HDACs act as specific performers determining the level and persistence of protein acetylation, including non-histone proteins. The use of ACSS2 inhibitors consistently downregulated the acetylation of H3 at lysine 9 and 27 in tumor cells, irrespective of whether they were under specific stresses or not. This alteration in histone binding to DNA inhibited numerous downstream gene expression and synthesis changes regulated by both. However, our analyses revealed no apparent mutual regulation between the increase in ACSS2 under nutritional stress and classical HAT proteins. Even though CBP and p300 was the core HATs explicitly involved in enhancing acetylation after ACSS2 upregulation, and both proteins showed slight fluctuations in the early stage of nutrient deprivation, there were no significant differences in these changes between HATs when histone H3 acetylation reached a stable stage. Additionally, in BC cells with low serum supply, HDAC4 showed a short period of suppression at the initial stage, and HDAC5 and HDAC8 also exhibited irregular fluctuations. However, the magnitude and duration of these changes were not consistent with

the persistent trend of H3K9ac and H3K27ac increase at the end of the treatment. These observations suggest that while there was evidence that elevated ACSS2 yieldeda significant acetylation-promoting effect on non-histone proteins, a more consistent phenomenon among BC cells was that ACSS2 was better focused on providing a steady stream of acetyl groups for histone acetylation in the nucleus[57–59]. Additionally, cancer cells under stress exhibited significant recruitment of the stabilizable form of ACSS2, p-ACSS2, in the nucleus upon acetate supplementation, in line with previous findings[18–20]. Our investigations established that ACSS2 in BC cells, while not a conventional acetyltransferase, and plays a role in promoting epigenetic activation downstream of H3K9/27 through its interaction with CBP/p300 in histone acetyltransferases. This process is mainly triggered by environmental stresses, with ACSS2 showing heightened sensitivity to nutrient stress. These findings suggest that ACSS2, expressed at high levels in cancer cells within BC tumors, may play a broader role in advancing further progression through its involvement in histone acetylation. Its impact extends beyond merely providing energy supply or serving as substrates for substance synthesis. Instead, ACSS2 appears to contribute significantly to the epigenetic regulation of gene expression via histone modifications, particularly in response to environmental stressors.

Recent studies on clear cell renal cancer have demonstrated that the knockdown of ACSS2 or the administration of ACSS2 inhibitors induces a transformation in tumor cells from being acetate mass consumers to becoming sustained suppliers of acetate production[60]. Similarly, targeting ACSS2 expression in TNBC cells not only intrinsically impedes tumor cell metabolism, particularly related to acetate but also enhances the ability of tumor-infiltrating T cells and NK cells to eliminate tumor cells. This is achieved by providing sufficient acetate to the tumor microenvironment[61]. The observed similarity suggests that both acetate synthesis and utilization, actively involving ACSS2 in tumor cells, are tightly dependent on transporters capable of intra- and extracellular substance uptake and transport. Despite differences in the magnitude of alterations between drug-specific targets and cell types, data from numerous tumor cells indicate that HDAC inhibitors such as TSA and SCFAs such as valproate (VPA) and butyrate, significantly modulate the expression and activity of MDR1 and BCRP[13, 62, 63]. It can be speculated that the ACSS2-induced histone H3K9/27 activation found in this study is functionally linked to the activity and expression of ATP-binding cassette transporters, which play a crucial role in energy metabolism and material transport. Results demonstrated that ACSS2 accumulation in BC cells after nutrient stress treatment could lead to the resynthesis of MDR1 and BCRP compared to cells under normal culture conditions. Altered levels directly limit the efficacy of chemotherapeutic agents for BC, such as Dox and DDP. To exclude the possibility that altered expression of MDR1 and BCRP might feedback to affect ACSS2 expression, the study showed that under identical stress conditions, single downregulation or combined inhibition of MDR1 and BCRP did not significantly affect ACSS2 expression but inhibited further histone acetylation. Recent research indicated that VPA supplementation could promote the expression of MDR1 and BCRP in the mouse brain's striatum by increasing histone acetylation levels. Similarly, VPA stimulation of acute myeloid leukemia cells has been observed to induce histone hyperacetylation in the promoter regions of MDR1 and BCRP[62, 64]. Furthermore, the histone acetylation modification process mediates the synthesis of ACSS2. However, data demonstrated that

inhibition of ABC transporter expression, with or without acetate addition, blocked histone H3 acetylation. Importantly, all of these interventions failed to effectively control ACSS2 expression, indicating that the presence and ability of MDR1 and BCRP to respond to intra- and extracellular stresses are crucial for maintaining cellular energy balance and metabolism. This highlights the complexity of epigenetic pharmacology among different types of tumors[56]. The observation of significant expression heterogeneity of ACSS2 among patients, as identified in our previous study on esophageal squamous cell carcinoma (ESCC), suggests a potential correlation with variations in individual gene expression, varying degrees of tumor progression, and dynamic changes in tumor microenvironments[36]. In the majority of BC patients examined in this study, the upregulation of ACSS2 was consistent with enhanced expression of MDR1 and BCRP, although differences existed in overall levels between different indicators or combinations. This variability allowed for a stratified analysis of patients based on their ACSS2 expression. When combined with the results of prognostic analysis, the overall 5-year survival rate was notably higher in the group of patients with lower ACSS2 levels. Independent studies across various cancers, including glioblastoma, BC, colon cancer, and melanoma, have demonstrated that targeted interference and inactivation of ACSS2 can inhibit tumor growth. The broad therapeutic scope underscores the significance of this enzyme in tumor progression[18–21, 23]. Restricting ACSS2 function can simultaneously control acetate utilization and synthesis, reducing the hyperactivation of histone acetylation under environmental stresses. This is partly dependent on alterations in the expression and function of MDR1 and BCRP. ACSS2 inhibitors show promise as epigenetic modulators that can enhance the effectiveness of chemotherapy. In combination with existing drugs, they may contribute to the elimination of refractory tumors and limit the emergence of drug resistance.

Conclusion

In conclusion, the findings reveal that BC cells reinforce the expression and function of efflux transporters in response to environmental stress through coordinated actions of metabolic enzymes, exemplified by ACSS2, and increased histone H3 acetylation. These novel mechanisms could be crucial for maintaining appropriate epigenetic and transcriptional regulation even when tumor cells undergo altered metabolic status.

Declarations

Acknowledgements We are grateful to the technical support from Shanghai Xiantaozi Data Technology Co., Ltd (www.xiantao.love) and acknowledge the contribution from TCGA database.

Author contributionsB.Z. planned, conceived and designed the experiments, and revised the manuscript. X.S. drafted the original manuscript. X.S., L.T., and Y.Z. conducted and performed all the experiments. X.S. and L.T. conducted statistical analysis. Y.Z. provided clinical samples and data. All the authors reviewed and approved the final manuscript.

Funding This work was supported by the Science Research Project of Hebei Education Department (No. QN2016180).

Competing interests The authors declare no competing interests.

Ethics approval and consent to participate All experimental procedures were performed in accordance with the Declaration of Helsinki and approved by the Institutional Review Board/Ethics Committee of Affiliated Hospital of Jiangsu University (KY2021K1213, Zhenjiang, China).

Consent for publication All authors have read the final manuscript and agreed for the publication.

References

1. Sung H, Ferlay J, Siegel RL, Laversanne M, Soerjomataram I, Jemal A, Bray F (2021) Global Cancer Statistics 2020: GLOBOCAN Estimates of Incidence and Mortality Worldwide for 36 Cancers in 185 Countries. CA Cancer J Clin 71:209–249. 10.3322/caac.21660
2. Azam A, Sounni NE (2022) Lipid Metabolism Heterogeneity and Crosstalk with Mitochondria Functions Drive Breast Cancer Progression and Drug Resistance. Cancers (Basel) 14. 10.3390/cancers14246267
3. Cao W, Chen HD, Yu YW, Li N, Chen WQ (2021) Changing profiles of cancer burden worldwide and in China: a secondary analysis of the global cancer statistics 2020. Chin Med J (Engl) 134:783–791. 10.1097/CM9.0000000000001474
4. Cao M, Li H, Sun D, Chen W (2020) Cancer burden of major cancers in China: A need for sustainable actions. Cancer Commun (Lond) 40:205–210. 10.1002/cac2.12025
5. Wang S, Zhou L, Ji N, Sun C, Sun L, Sun J, Du Y, Zhang N, Li Y, Liu W, Lu W (2023) Targeting ACYP1-mediated glycolysis reverses lenvatinib resistance and restricts hepatocellular carcinoma progression. Drug Resist Updat 69:100976. 10.1016/j.drup.2023.100976
6. Chen X, Luo R, Zhang Y, Ye S, Zeng X, Liu J, Huang D, Liu Y, Liu Q, Luo ML, Song E (2022) Long noncoding RNA DIO3OS induces glycolytic-dominant metabolic reprogramming to promote aromatase inhibitor resistance in breast cancer. Nat Commun 13:7160. 10.1038/s41467-022-34702-x
7. Li Q, Qin T, Bi Z, Hong H, Ding L, Chen J, Wu W, Lin X, Fu W, Zheng F, Yao Y, Luo ML, Saw PE, Wulf GM, Xu X, Song E, Yao H, Hu H (2020) Rac1 activates non-oxidative pentose phosphate pathway to induce chemoresistance of breast cancer. Nat Commun 11:1456. 10.1038/s41467-020-15308-7
8. Yoon BK, Kim H, Oh TG, Oh SK, Jo S, Kim M, Chun KH, Hwang N, Lee S, Jin S, Atkins AR, Yu RT, Downes M, Kim JW, Kim H, Evans RM, Cheong JH, Fang S (2023) PHGDH preserves one-carbon cycle to confer metabolic plasticity in chemoresistant gastric cancer during nutrient stress. Proc Natl Acad Sci U S A 120:e2217826120. 10.1073/pnas.2217826120
9. Sher G, Salman NA, Khan AQ, Prabhu KS, Raza A, Kulinski M, Dermime S, Haris M, Junejo K, Uddin S (2022) Epigenetic and breast cancer therapy: Promising diagnostic and therapeutic applications.

Semin Cancer Biol 83:152–165. 10.1016/j.semcancer.2020.08.009

10. Wang X, Xu J, Sun Y, Cao S, Zeng H, Jin N, Shou M, Tang S, Chen Y, Huang M (2023) Hedgehog pathway orchestrates the interplay of histone modifications and tailors combination epigenetic therapies in breast cancer. Acta Pharm Sin B 13:2601–2612. 10.1016/j.apsb.2023.03.009
11. Toth M, Boros IM, Balint E (2012) Elevated level of lysine 9-acetylated histone H3 at the MDR1 promoter in multidrug-resistant cells. Cancer Sci 103:659–669. 10.1111/j.1349-7006.2012.02215.x
12. Strachowska M, Gronkowska K, Michlewska S, Robaszkiewicz A (2021) CBP/p300 Bromodomain Inhibitor-I-CBP112 Declines Transcription of the Key ABC Transporters and Sensitizes Cancer Cells to Chemotherapy Drugs. Cancers (Basel) 13. 10.3390/cancers13184614
13. Xie QS, Zhang JX, Liu M, Liu PH, Wang ZJ, Zhu L, Jiang L, Jin MM, Liu XN, Liu L, Liu XD (2021) Short-chain fatty acids exert opposite effects on the expression and function of p-glycoprotein and breast cancer resistance protein in rat intestine. Acta Pharmacol Sin 42:470–481. 10.1038/s41401-020-0402-x
14. Martinez Calejman C, Trefely S, Entwisle SW, Luciano A, Jung SM, Hsiao W, Torres A, Hung CM, Li H, Snyder NW, Villen J, Wellen KE, Guertin (2020) DA mTORC2-AKT signaling to ATP-citrate lyase drives brown adipogenesis and de novo lipogenesis. Nat Commun 11:575. 10.1038/s41467-020-14430-w
15. Hao F, Tian M, Zhang X, Jin X, Jiang Y, Sun X, Wang Y, Peng P, Liu J, Xia C, Feng Y, Wei M (2021) Butyrate enhances CPT1A activity to promote fatty acid oxidation and iTreg differentiation. Proc Natl Acad Sci U S A 118. 10.1073/pnas.2014681118
16. Han A, Bennett N, MacDonald A, Johnstone M, Whelan J, Donohoe DR (2016) Cellular Metabolism and Dose Reveal Carnitine-Dependent and -Independent Mechanisms of Butyrate Oxidation in Colorectal Cancer Cells. J Cell Physiol 231:1804–1813. 10.1002/jcp.25287
17. You D, Richardson JR, Aleksunes LM (2020) Epigenetic Regulation of Multidrug Resistance Protein 1 and Breast Cancer Resistance Protein Transporters by Histone Deacetylase Inhibition. Drug Metab Dispos 48:459–480. 10.1124/dmd.119.089953
18. Ciraku L, Bacigalupa ZA, Ju J, Moeller RA, Le Minh G, Lee RH, Smith MD, Ferrer CM, Trefely S, Izzo LT, Doan MT, Gocal WA, D'Agostino L, Shi W, Jackson JG, Katsetos CD, Wellen KE, Snyder NW, Reginato MJ (2022) O-GlcNAc transferase regulates glioblastoma acetate metabolism via regulation of CDK5-dependent ACSS2 phosphorylation. Oncogene 41:2122–2136. 10.1038/s41388-022-02237-6
19. Li X, Qian X, Lu Z (2017) Local histone acetylation by ACSS2 promotes gene transcription for lysosomal biogenesis and autophagy. Autophagy 13:1790–1791. 10.1080/15548627.2017.1349581
20. Li X, Yu W, Qian X, Xia Y, Zheng Y, Lee JH, Li W, Lyu J, Rao G, Zhang X, Qian CN, Rozen SG, Jiang T, Lu Z (2017) Nucleus-Translocated ACSS2 Promotes Gene Transcription for Lysosomal Biogenesis and Autophagy. Mol Cell 66(e9):684–697. 10.1016/j.molcel.2017.04.026
21. Miller KD, Pniewski K, Perry CE, Papp SB, Shaffer JD, Velasco-Silva JN, Casciano JC, Aramburu TM, Srikanth YVV, Cassel J, Skordalakes E, Kossenkov AV, Salvino JM, Schug ZT (2021) Targeting ACSS2 with a Transition-State Mimetic Inhibits Triple-Negative Breast Cancer Growth. Cancer Res 81:1252–1264. 10.1158/0008-5472.CAN-20-1847

22. Izzo LT, Trefely S, Demetriadou C, Drummond JM, Mizukami T, Kuprasertkul N, Farria AT, Nguyen PTT, Murali N, Reich L, Kantner DS, Shaffer J, Affronti H, Carrer A, Andrews A, Capell BC, Snyder NW, Wellen KE (2023) Acetylcarnitine shuttling links mitochondrial metabolism to histone acetylation and lipogenesis. Sci Adv 9:eadf0115. 10.1126/sciadv.adf0115
23. Garcia JA, Chen R, Xu M, Comerford SA, Hammer RE, Melton SD, Feagins LA (2023) Acss2/HIF-2 signaling facilitates colon cancer growth and metastasis. PLoS ONE 18:e0282223. 10.1371/journal.pone.0282223
24. Kondo A, Yamamoto S, Nakaki R, Shimamura T, Hamakubo T, Sakai J, Kodama T, Yoshida T, Aburatani H, Osawa T (2017) Extracellular Acidic pH Activates the Sterol Regulatory Element-Binding Protein 2 to Promote Tumor Progression. Cell Rep 18:2228–2242. 10.1016/j.celrep.2017.02.006
25. Bulusu V, Tumanov S, Michalopoulou E, van den Broek NJ, MacKay G, Nixon C, Dhayade S, Schug ZT, Vande Voorde J, Blyth K, Gottlieb E, Vazquez A, Kamphorst JJ (2017) Acetate Recapturing by Nuclear Acetyl-CoA Synthetase 2 Prevents Loss of Histone Acetylation during Oxygen and Serum Limitation. Cell Rep 18:647–658. 10.1016/j.celrep.2016.12.055
26. Zheng J, Zhang YF, Han GH, Fan MY, Du MH, Zhang GC, Zhang B, Qiao J, Zhang SX, Cao JM (2023) Identification and Validation of a Novel Glycolysis-Related Gene Signature for Predicting the Prognosis and Therapeutic Response in Triple-Negative Breast Cancer. Adv Ther 40:310–330. 10.1007/s12325-022-02330-y
27. Wu Z, Han T, Su H, Xuan J, Wang X (2022) Comprehensive analysis of fatty acid and lactate metabolism-related genes for prognosis value, immune infiltration, and therapy in osteosarcoma patients. Front Oncol 12:934080. 10.3389/fonc.2022.934080
28. Zhang S, He J, Jia Z, Yan Z, Yang J (2018) Acetyl-CoA synthetase 2 enhances tumorigenesis and is indicative of a poor prognosis for patients with renal cell carcinoma. Urol Oncol 36:243 e9-243 e20. 10.1016/j.urolonc.2018.01.013
29. Sun L, Kong Y, Cao M, Zhou H, Li H, Cui Y, Fang F, Zhang W, Li J, Zhu X, Li Q, Song T, Zhang T (2017) Decreased expression of acetyl-CoA synthase 2 promotes metastasis and predicts poor prognosis in hepatocellular carcinoma. Cancer Sci 108:1338–1346. 10.1111/cas.13252
30. Hur H, Kim YB, Ham IH, Lee D (2015) Loss of ACSS2 expression predicts poor prognosis in patients with gastric cancer. J Surg Oncol 112:585–591. 10.1002/jso.24043
31. Liang Y, Yi L, Deng P, Wang L, Yue Y, Wang H, Tian L, Xie J, Chen M, Luo Y, Yu Z, Pi H, Zhou Z (2021) Rapamycin antagonizes cadmium-induced breast cancer cell proliferation and metastasis through directly modulating ACSS2. Ecotoxicol Environ Saf 224:112626. 10.1016/j.ecoenv.2021.112626
32. Liang Y, Pi H, Liao L, Tan M, Deng P, Yue Y, Xi Y, Tian L, Xie J, Chen M, Luo Y, Chen M, Wang L, Yu Z, Zhou Z (2021) Cadmium promotes breast cancer cell proliferation, migration and invasion by inhibiting ACSS2/ATG5-mediated autophagy. Environ Pollut 273:116504. 10.1016/j.envpol.2021.116504
33. Calhoun S, Duan L, Maki CG (2022) Acetyl-CoA synthetases ACSS1 and ACSS2 are 4-hydroxytamoxifen responsive factors that promote survival in tamoxifen treated and estrogen

deprived cells. Transl Oncol 19:101386. 10.1016/j.tranon.2022.101386

34. Schug ZT, Peck B, Jones DT, Zhang Q, Grosskurth S, Alam IS, Goodwin LM, Smethurst E, Mason S, Blyth K, McGarry L, James D, Shanks E, Kalna G, Saunders RE, Jiang M, Howell M, Lassailly F, Thin MZ, Spencer-Dene B, Stamp G, van den Broek NJ, Mackay G, Bulusu V, Kamphorst JJ, Tardito S, Strachan D, Harris AL, Aboagye EO, Critchlow SE, Wakelam MJ, Schulze A, Gottlieb E (2015) Acetyl-CoA synthetase 2 promotes acetate utilization and maintains cancer cell growth under metabolic stress. Cancer Cell 27:57–71. 10.1016/j.ccell.2014.12.002
35. Comerford SA, Huang Z, Du X, Wang Y, Cai L, Witkiewicz AK, Walters H, Tantawy MN, Fu A, Manning HC, Horton JD, Hammer RE, McKnight SL, Tu BP (2014) Acetate dependence of tumors. Cell 159:1591–1602. 10.1016/j.cell.2014.11.020
36. Mi L, Zhou Y, Wu D, Tao Q, Wang X, Zhu H, Gao X, Wang J, Ling R, Deng J, Mao C, Chen D (2019) ACSS2/AMPK/PCNA pathway–driven proliferation and chemoresistance of esophageal squamous carcinoma cells under nutrient stress. Mol Med Rep 20:5286–5296. 10.3892/mmr.2019.10735
37. Yu WS, Jeong SJ, Kim JH, Lee HJ, Song HS, Kim MS, Ko E, Lee HJ, Khil JH, Jang HJ, Kim YC, Bae H, Chen CY, Kim SH (2011) The genome-wide expression profile of 1,2,3,4,6-penta-O-galloyl-beta-D-glucose-treated MDA-MB-231 breast cancer cells: molecular target on cancer metabolism. Mol Cells 32:123 – 32. 10.1007/s10059-011-2254-1
38. Kappler M, Pabst U, Weinholdt C, Taubert H, Rot S, Kaune T, Kotrba J, Porsch M, Guttler A, Bache M, Krohn K, Bull F, Riemann A, Wickenhauser C, Seliger B, Schubert J, Al-Nawas B, Thews O, Grosse I, Vordermark D, Eckert AW (2019) Causes and Consequences of A Glutamine Induced Normoxic HIF1 Activity for the Tumor Metabolism. Int J Mol Sci 20. 10.3390/ijms20194742
39. Mittal L, Aryal UK, Camarillo IG, Ferreira RM, Sundararajan R (2019) Quantitative proteomic analysis of enhanced cellular effects of electrochemotherapy with Cisplatin in triple-negative breast cancer cells. Sci Rep 9:13916. 10.1038/s41598-019-50048-9
40. Li X, Zhou C, Qiu C, Li W, Yu Q, Huang H, Zhang Y, Zhang X, Ren L, Huang X, Zhou Q (2022) A cholesterogenic gene signature for predicting the prognosis of young breast cancer patients. PeerJ 10:e13922. 10.7717/peerj.13922
41. Purrington KS, Gorski D, Simon MS, Hastert TA, Kim S, Rosati R, Schwartz AG, Ratnam M (2020) Racial differences in estrogen receptor staining levels and implications for treatment and survival among estrogen receptor positive, HER2-negative invasive breast cancers. Breast Cancer Res Treat 181:145–154. 10.1007/s10549-020-05607-4
42. Bauer KR, Brown M, Cress RD, Parise CA, Caggiano V (2007) Descriptive analysis of estrogen receptor (ER)-negative, progesterone receptor (PR)-negative, and HER2-negative invasive breast cancer, the so-called triple-negative phenotype: a population-based study from the California cancer Registry. Cancer 109:1721–1728. 10.1002/cncr.22618
43. Que D, Kuang F, Kang R, Tang D, Liu J (2023) ACSS2-mediated NF-kappaB activation promotes alkaliptosis in human pancreatic cancer cells. Sci Rep 13:1483. 10.1038/s41598-023-28261-4

44. Anderson R, Pladna KM, Schramm NJ, Wheeler FB, Kridel S, Pardee TS (2023) Pyruvate Dehydrogenase Inhibition Leads to Decreased Glycolysis, Increased Reliance on Gluconeogenesis and Alternative Sources of Acetyl-CoA in Acute Myeloid Leukemia. Cancers (Basel) 15. 10.3390/cancers15020484
45. Li Z, Liu H, He J, Wang Z, Yin Z, You G, Wang Z, Davis RE, Lin P, Bergsagel PL, Manasanch EE, Wong STC, Esnaola NF, Chang JC, Orlowski RZ, Yi Q, Yang J (2021) Acetyl-CoA Synthetase 2: A Critical Linkage in Obesity-Induced Tumorigenesis in Myeloma. Cell Metab 33:78–93e7. 10.1016/j.cmet.2020.12.011
46. Ni Y, Yang Y, Ran J, Zhang L, Yao M, Liu Z, Zhang L (2020) miR-15a-5p inhibits metastasis and lipid metabolism by suppressing histone acetylation in lung cancer. Free Radic Biol Med 161:150–162. 10.1016/j.freeradbiomed.2020.10.009
47. Martinez-Chavez A, Loos NHC, Lebre MC, Tibben MM, Rosing H, Beijnen JH, Schinkel AH (2022) ABCB1 and ABCG2 limit brain penetration and, together with CYP3A4, total plasma exposure of abemaciclib and its active metabolites. Pharmacol Res 178:105954. 10.1016/j.phrs.2021.105954
48. Rendic SP (2021) Metabolism and interactions of Ivermectin with human cytochrome P450 enzymes and drug transporters, possible adverse and toxic effects. Arch Toxicol 95:1535–1546. 10.1007/s00204-021-03025-z
49. Lasko LM, Jakob CG, Edalji RP, Qiu W, Montgomery D, Digiammarino EL, Hansen TM, Risi RM, Frey R, Manaves V, Shaw B, Algire M, Hessler P, Lam LT, Uziel T, Faivre E, Ferguson D, Buchanan FG, Martin RL, Torrent M, Chiang GG, Karukurichi K, Langston JW, Weinert BT, Choudhary C, de Vries P, Van Drie JH, McElligott D, Kesicki E, Marmorstein R, Sun C, Cole PA, Rosenberg SH, Michaelides MR, Lai A, Bromberg KD (2017) Discovery of a selective catalytic p300/CBP inhibitor that targets lineage-specific tumours. Nature 550:128–132. 10.1038/nature24028
50. Guertin DA, Wellen KE (2023) Acetyl-CoA metabolism in cancer. Nat Rev Cancer 23:156–172. 10.1038/s41568-022-00543-5
51. Zhang L, McCabe T, Condra JH, Ni YG, Peterson LB, Wang W, Strack AM, Wang F, Pandit S, Hammond H, Wood D, Lewis D, Rosa R, Mendoza V, Cumiskey AM, Johns DG, Hansen BC, Shen X, Geoghagen N, Jensen K, Zhu L, Wietecha K, Wisniewski D, Huang L, Zhao JZ, Ernst R, Hampton R, Haytko P, Ansbro F, Chilewski S, Chin J, Mitnaul LJ, Pellacani A, Sparrow CP, An Z, Strohl W, Hubbard B, Plump AS, Blom D, Sitlani A (2012) An anti-PCSK9 antibody reduces LDL-cholesterol on top of a statin and suppresses hepatocyte SREBP-regulated genes. Int J Biol Sci 8:310–327. 10.7150/ijbs.3524
52. Xu H, Luo J, Ma G, Zhang X, Yao D, Li M, Loor JJ (2018) Acyl-CoA synthetase short-chain family member 2 (ACSS2) is regulated by SREBP-1 and plays a role in fatty acid synthesis in caprine mammary epithelial cells. J Cell Physiol 233:1005–1016. 10.1002/jcp.25954
53. Chen C, Chen W, Ding H, Wu P, Zhang G, Xie K, Zhang T (2023) High-fat diet-induced gut microbiota alteration promotes lipogenesis by butyric acid/miR-204/ACSS2 axis in chickens. Poult Sci 102:102856. 10.1016/j.psj.2023.102856

54. Kang Z, Zhang S, Jiang E, Wan F, Lan X, Liu M (2020) Mir-193b Regulates the Differentiation, Proliferation, and Apoptosis of Bovine Adipose Cells by Targeting the ACSS2/AKT Axis. Anim (Basel) 10. 10.3390/ani10081265
55. Gan S, Mao J, Pan Y, Tang J, Qiu Z (2021) hsa-miR-15b-5p regulates the proliferation and apoptosis of human vascular smooth muscle cells by targeting the ACSS2/PTGS2 axis. Exp Ther Med 22:1208. 10.3892/etm.2021.10642
56. Gao X, Lin SH, Ren F, Li JT, Chen JJ, Yao CB, Yang HB, Jiang SX, Yan GQ, Wang D, Wang Y, Liu Y, Cai Z, Xu YY, Chen J, Yu W, Yang PY, Lei QY (2016) Acetate functions as an epigenetic metabolite to promote lipid synthesis under hypoxia. Nat Commun 7:11960. 10.1038/ncomms11960
57. Nagati JS, Kobeissy PH, Nguyen MQ, Xu M, Garcia T, Comerford SA, Hammer RE, Garcia JA (2021) Mammalian acetate-dependent acetyl CoA synthetase 2 contains multiple protein destabilization and masking elements. J Biol Chem 297:101037. 10.1016/j.jbc.2021.101037
58. Nagati JS, Xu M, Garcia T, Comerford SA, Hammer RE, Garcia JA (2019) A substitution mutation in a conserved domain of mammalian acetate-dependent acetyl CoA synthetase 2 results in destabilized protein and impaired HIF-2 signaling. PLoS ONE 14:e0225105. 10.1371/journal.pone.0225105
59. Chen R, Xu M, Nagati JS, Hogg RT, Das A, Gerard RD, Garcia JA (2015) The acetate/ACSS2 switch regulates HIF-2 stress signaling in the tumor cell microenvironment. PLoS ONE 10:e0116515. 10.1371/journal.pone.0116515
60. Bacigalupa ZA, Brown WA, Krystofiak ES, Wolf MM, Hongo RA, Landis M, Amason EK, Beckermann KE, Rathmell JC, Rathmell WK (2022) ACSS2 Regulates HIF-2α Degradation through the E3-Ubiquitin Ligase MUL1 in Clear Cell Renal Cell Carcinoma. Preprint at bioRxiv. 10.1101/2022.04.21.489116
61. Miller KD, O'Connor S, Pniewski KA, Kannan T, Acosta R, Mirji G, Papp S, Hulse M, Mukha D, Hlavaty SI, Salcido KN, Bertolazzi F, Srikanth YVV, Zhao S, Wellen KE, Shinde RS, Claiborne DT, Kossenkov A, Salvino JM, Schug ZT (2023) Acetate acts as a metabolic immunomodulator by bolstering T-cell effector function and potentiating antitumor immunity in breast cancer. Nat Cancer. 10.1038/s43018-023-00636-6
62. You D, Shin HM, Mosaad F, Richardson JR, Aleksunes LM (2019) Brain region-specific regulation of histone acetylation and efflux transporters in mice. J Biochem Mol Toxicol 33:e22318. 10.1002/jbt.22318
63. Hauswald S, Duque-Afonso J, Wagner MM, Schertl FM, Lubbert M, Peschel C, Keller U, Licht T (2009) Histone deacetylase inhibitors induce a very broad, pleiotropic anticancer drug resistance phenotype in acute myeloid leukemia cells by modulation of multiple ABC transporter genes. Clin Cancer Res 15:3705–3715. 10.1158/1078-0432.CCR-08-2048
64. Tang R, Faussat AM, Majdak P, Perrot JY, Chaoui D, Legrand O, Marie JP (2004) Valproic acid inhibits proliferation and induces apoptosis in acute myeloid leukemia cells expressing P-gp and MRP1. Leukemia 18:1246–1251. 10.1038/sj.leu.2403390

Figures

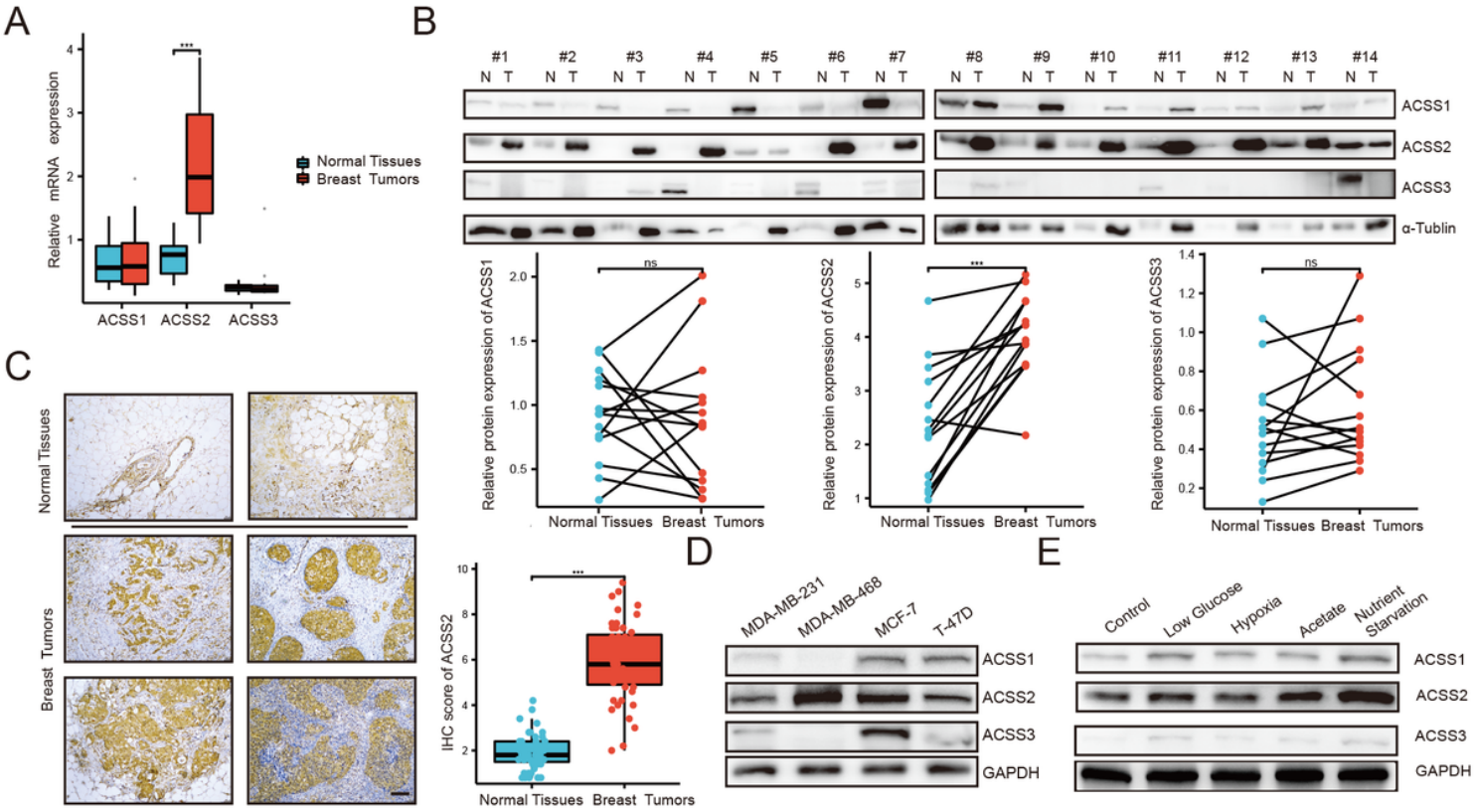

Figure 1

ACSS2 is upregulated in BC tumors and cells. A Results of the RT-PCR analysis of 14 pairs of BC tumors and adjacent normal tissues. B Representative images and statistical analysis of the Western blotting of 14 pairs of BC tumors and adjacent normal tissues. N, normal tissues. T, BC tumors. C Typical IHC images and statistical analysis of ACSS2 expression status in 47 pairs of adjacent normal breast tissues and BC tumors. Scale bars, 200 μm. D Western blot analysis results validated the expression of ACSS family members in MDA-MB-231, MDA-MB-468, MCF-7 and T-47D cells. E Western blot analysis of ACSS1, ACSS2 and ACSS3 expression in T-47D cells with the indicated treatment. Low Glucose (the glucose concentration is 1 g/L, 48 h), Hypoxia (the oxygen concentration at 1% for 7 days), Acetate (0.5 mM, 24 h), Nutrient Starvation (1%FBS, 48 h). The error bars represent the mean ± SD. $^{*}P < 0.05$, $^{**}P < 0.01$, $^{***}P < 0.001$. ns means non-significant.

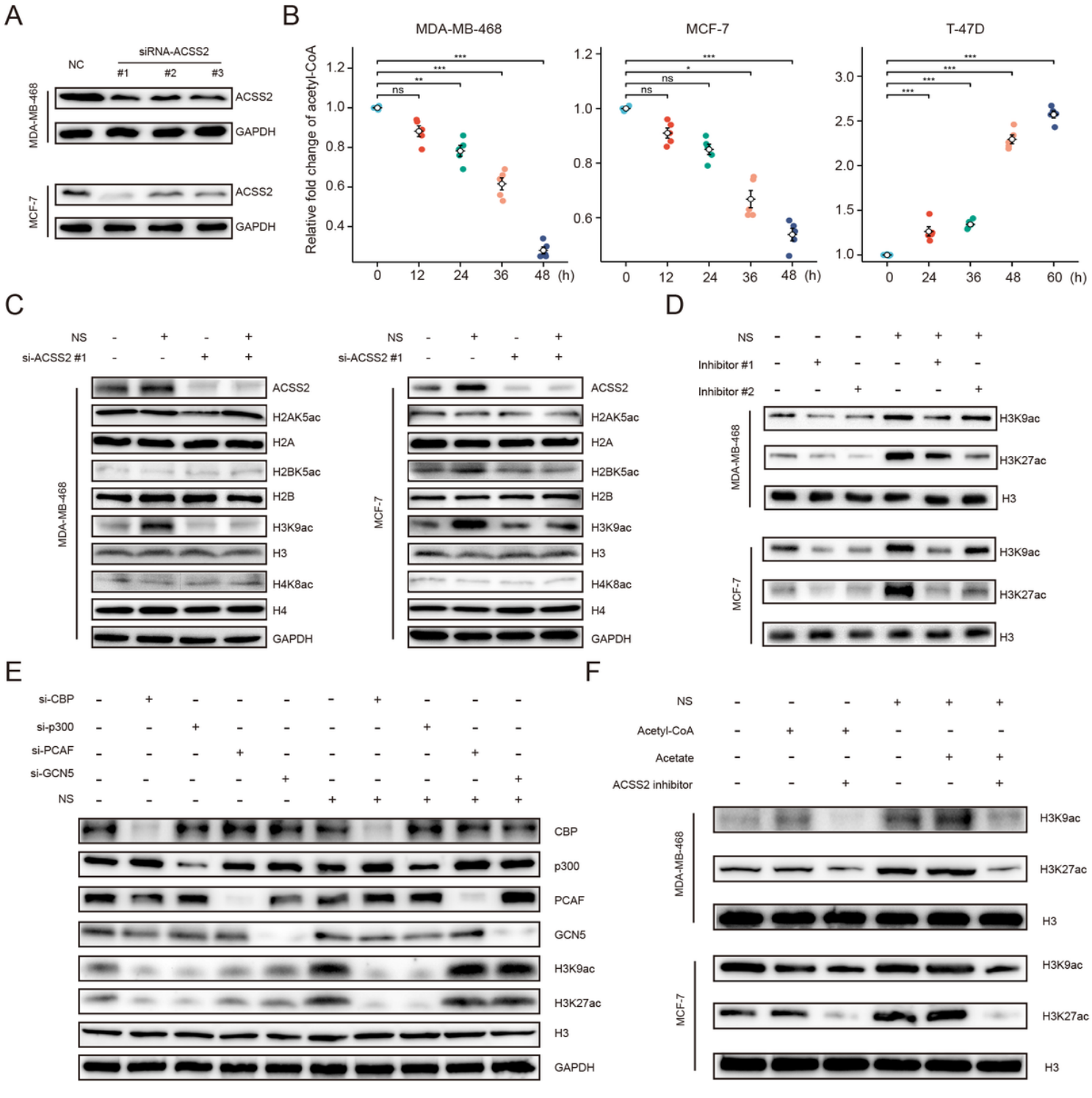

Figure 2

ACSS2 induced the accumulation of acetyl-CoA and upregulate histone H3 acetylation. A The MDA-MB-468 and MCF-7 cells were transfected with negative control (NC) or three independent ACSS2 siRNAs (siRNA-ACSS2) for 48 hours. The effects of targeted interference were detected by Western blot analysis. B The indicated cells were treated with siRNA-ACSS2 (MDA-MB-468 and MCF-7 cells) or over-expression of ACSS2 (T-47D cells) for time gradient. Cell lysates were then extracted and subjected to ELISA analysis. Graph reporting the fold changes of acetyl-CoA levels. C MDA-MB-468 and MCF-7 cells with

ACSS2 reduction were cultured under nutrient stress (NS, 48 hours) or not. The expression of ACSS2, acetylated histones and total histones were detected by Western blotting. D BC cells pretreated with different ACSS2 inhibitors (#1, ACSS2 inhibitors, 5 μM and #2, VY-3-135, 50 nM) were cultured in medium with l% FBS for 48 h, and acetylated histone H3 were then measured. E Modulation of the HATs and ACSS2 expression in MDA-MB-468 cells before and after NS treatment were validated by RNA interference. si-CBP, siRNA-CBP. si-p300, siRNA-p300. si-PCAF, siRNA-PCAF. si-GCN5, siRNA-GCN5. F The change of histone H3 acetylation of BC cells, respectively combined with NS (48 hours), ACSS2 inhibitor (5.0 μM, 8 hours), the supplement of acetyl-CoA (1 μM, 2 hours) and acetate (0.5 mM, 2 hours), were assessed by Western blotting. The error bars represent the mean ± SD. $^{*}P < 0.05$, $^{**}P < 0.01$, $^{***}P < 0.001$, and ns means non-significant.

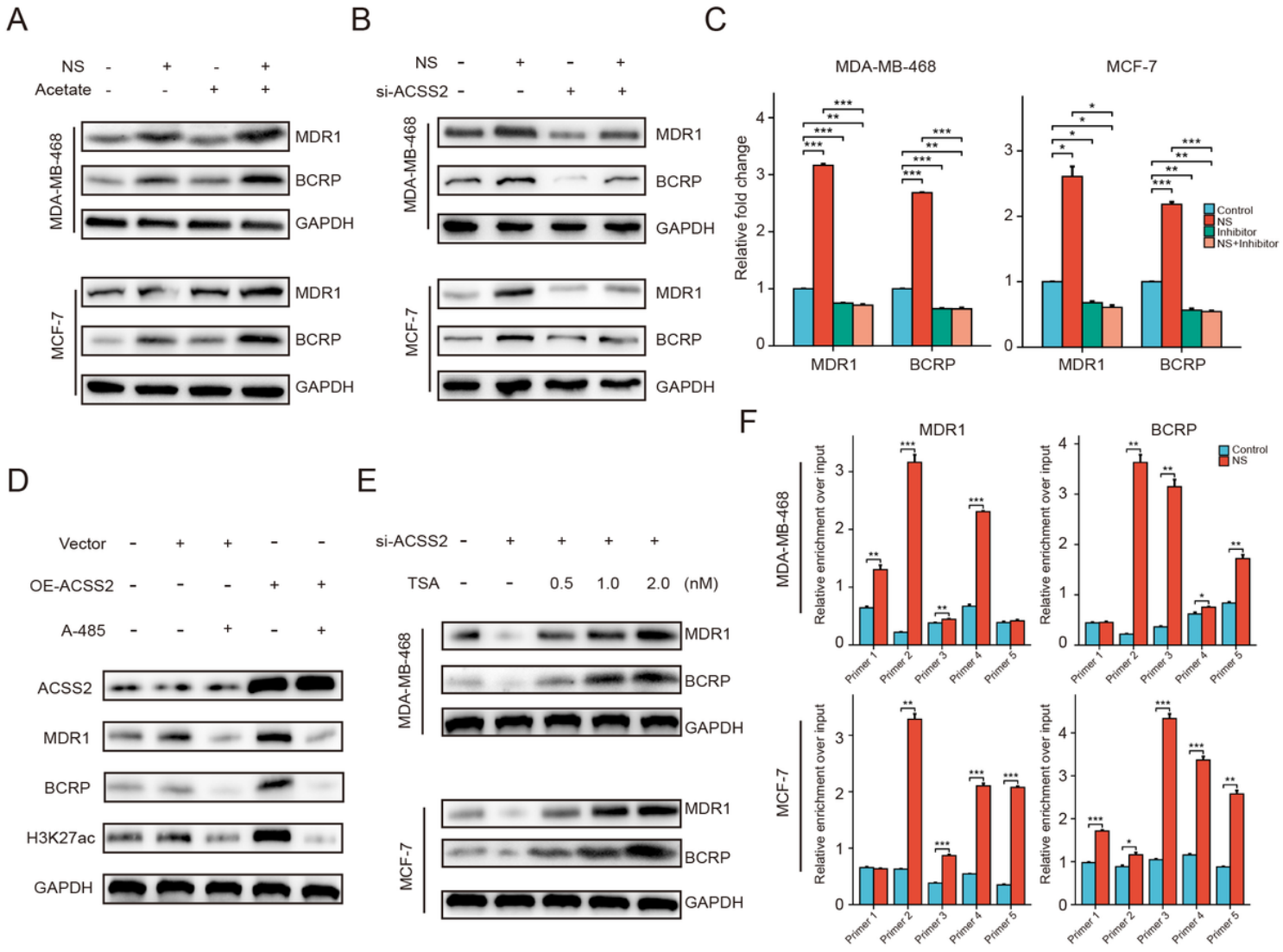

Figure 3

ACSS2 induces the expression of ABC transporters depend on the acetylated histones H3. A Western blot analysis of ABC transporters (MDR1 and BCRP) expression in BC cells treated or not acetate (0.5 mM, 12 hours) for 48 hours under nutrient stress as indicated. B Western blot analysis of MDR1 and BCRP

expression in MDA-MB-468 and MCF-7 cells silenced for ACSS2 and then treated or not with nutrient stress for 48 hours. C MDA-MB-468 and MCF-7 cells were treated or not with nutrient stress for 48 hours, and/or ACSS2 inhibitor (5 μM) for another 12 hours. The mRNA levels of MDR1 and BCRP were measured. D T-47D cells transfected with either empty vectors or vectors expressing ACSS2 in combination or not A-485 (5 μM) for 6 hours. Lysates were harvested 48 hours after treatment. E Representative images of BC cells transduced with control or siRNA-ACSS2 (si-ACSS2) for 24 hours, and treated with increasing dose of TSA for 12 hours. F ChIP assay demonstrated that H3K27 acetylation occurred in the promoter of MDR1 and BCRP in BC cell lines using five primers upon treatment of nutrient stress (48 hours). The error bars represent the mean ± SD. $^{*}P < 0.05$, $^{**}P < 0.01$, $^{***}P < 0.001$.

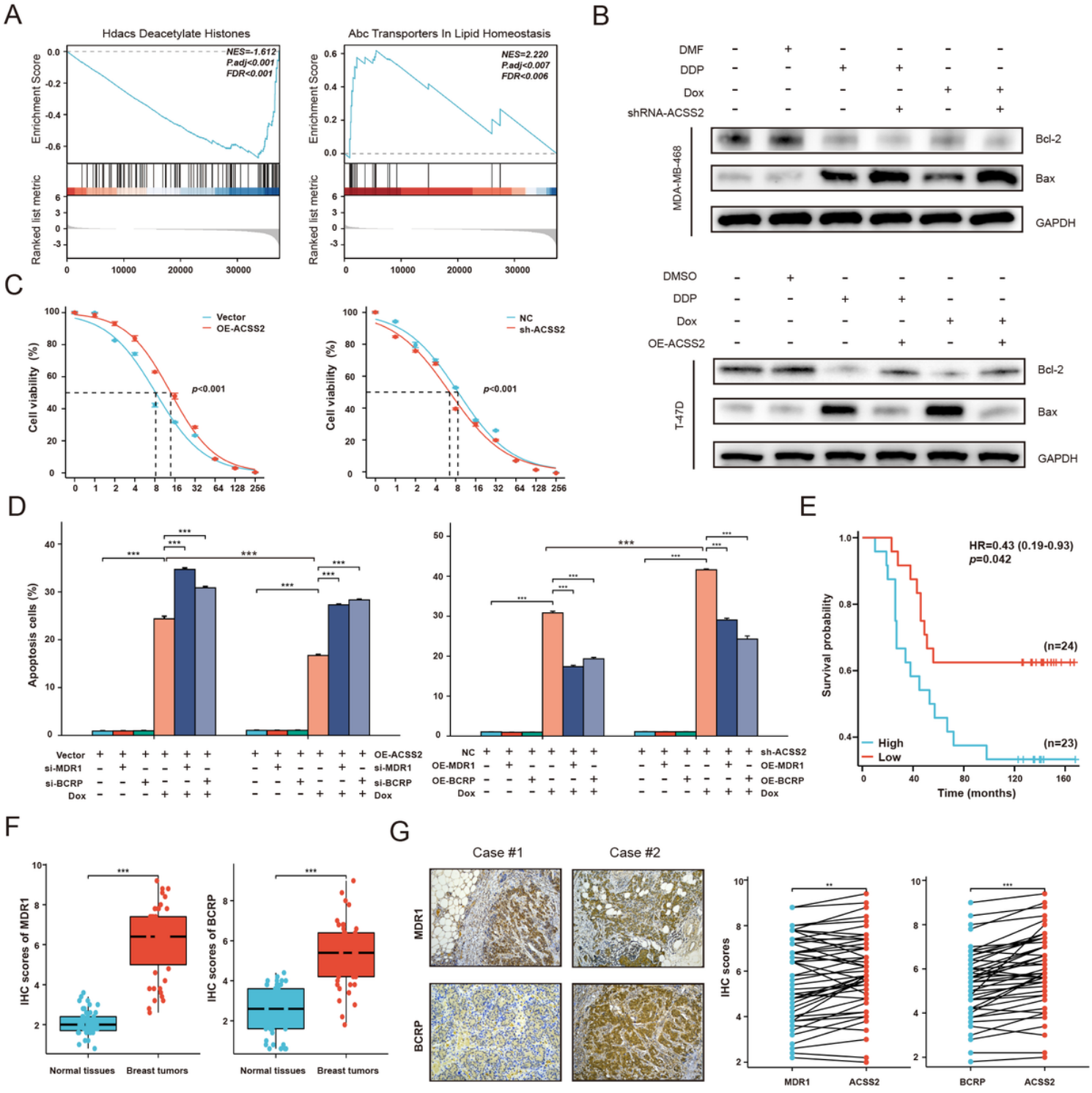

Figure 4

ACSS2 desensitizes BC to drugs and its upregulation predicts poor prognosis. A GSEA plot showing that the correlation of ACSS2 expression with HDAC deacetylate and ABC transporters levels in BC. B The indicated cells were treated with 5 nM Dox or 5 mM DDP for 24 hours. Cell lysates were then extracted, and the expression of genes related to apoptosis were detected by Western blotting. C MCF-7 (left) and MDA-MB-468 (right) cells transfected with the indicated constructs were treated with Dox (0, 1, 2, 4, 8, 16, 32, 64, 128, 256 nM) for 24 hours and then and the change of IC50 value were analyzed by CCK-8 assays.

D Apoptosis was measured by Annexin V detection. Flow cytometry results showing the effect of ACSS2 on apoptosis progression. E Kaplan-Meier analysis of OS according to ACSS2 expression status in 47 BC patients. F The statistical analysis of MDR1 and BCRP expression in 47 pairs of breast tissues and BC tumors. G Representative IHC staining images of MDR1 and BCRP in two BC samples (left). Statistical analysis of the correlation between MDR1or BCRP and ACSS2 expression levels detected by IHC staining (right). The error bars represent the mean ± SD. $^{*}P < 0.05$, $^{**}P < 0.01$, $^{***}P < 0.001$.

Supplementary Files

This is a list of supplementary files associated with this preprint. Click to download.

- Supplementarydata.docx